

# Reduced Model for Gravitational Wave Sources

A Thesis  
Presented to  
The Academic Faculty

by

**Lorena Magaña Zertuche**

In Partial Fulfillment  
of the Requirements for the Degree  
B.S. in Physics with the Research Option

School of Physics  
Georgia Institute of Technology  
May 2015

# Reduced Model for Gravitational Wave Sources

Approved by:

Professor Deirdre Shoemaker, Advisor  
Director, Center for Relativistic Astrophysics  
*Georgia Institute of Technology*

Professor Pablo Laguna  
Chair, School of Physics  
*Georgia Institute of Technology*

*To my family*

## ACKNOWLEDGEMENTS

I want to thank my supervisor, Prof. Deirdre Shoemaker, for allowing me to join her research group at an early stage in my undergraduate career and for her guidance throughout. I also thank her for being a mentor and friend. My appreciation goes towards Prof. Pablo Laguna for his helpful conversations and advice. Additionally, I thank Jim Healy who helped setup this project for me from the beginning and to Larne Pekowsky who developed code for my research purposes, for reviewing my code, and for answering questions at any time of the day. Thank you to James Clark who helped set up the stage for the future work. Additionally, I would like to thank Karan Jani for providing the figures of the spacetimes for both precessing series.

# TABLE OF CONTENTS

<b>DEDICATION</b> . . . . .	<b>iii</b>
<b>ACKNOWLEDGEMENTS</b> . . . . .	<b>iv</b>
<b>LIST OF FIGURES</b> . . . . .	<b>vi</b>
<b>ABSTRACT</b> . . . . .	<b>vii</b>
<b>I INTRODUCTION</b> . . . . .	<b>1</b>
<b>II NUMERICAL RELATIVITY</b> . . . . .	<b>3</b>
2.1 What is Numerical Relativity? . . . . .	3
2.2 Einstein's Equations . . . . .	4
2.3 Gravitational Waves . . . . .	5
2.4 Gauge Transformation . . . . .	6
<b>III ENERGY RADIATED</b> . . . . .	<b>8</b>
3.1 Theoretical Derivation . . . . .	8
3.2 Additional Corrections . . . . .	10
<b>IV DETECTION METHODS</b> . . . . .	<b>11</b>
4.1 LIGO . . . . .	11
4.2 Matched Filtering . . . . .	12
4.3 Principal Component Analysis . . . . .	12
<b>V RESULTS</b> . . . . .	<b>14</b>
5.1 Non-Precessing Binaries . . . . .	15
5.2 Precessing Binaries . . . . .	17
<b>VI CONCLUSIONS &amp; FUTURE WORK</b> . . . . .	<b>20</b>

# LIST OF FIGURES

4.1	Basic schematic of the LIGO interferometer. . . . .	12
5.1	A gravitational waveform where the y-axis represents the gravitational wave amplitude and the x-axis represents the time evolution of the binary black hole system merging. . . . .	14
5.2	The energy radiated by mass ratio, $q$ . . . . .	15
5.3	Energy decomposed into the three most dominant modes for non-spinning systems with a curve fit used for extrapolation. . . . .	16
5.4	Sketch of the initial parameters for a given spacetime setup and all the varying parameters, such as mass ratio $q$ . The colors represent different spin angles but same spin magnitudes $a_1$ and $a_2$ . . . . .	17
5.5	Energy radiated by mass ratio with a varying precession angle for systems of spin 0.6 with only the spin vector of the larger black hole changing. . . .	18
5.6	Sketch of the initial parameters for a given spacetime setup and all the varying parameters, such as mass ratio $q$ . The colors represent opposite spin angles but same spin magnitudes $a_1$ and $a_2$ . . . . .	19
5.7	Energy radiated by mass ratio with a varying precession angle for systems of spin 0.6 with spin vectors of each black hole pointing in opposite directions. . . .	19

# ABSTRACT

One of the most interesting and exotic systems in the universe is a system of two black holes. When black holes orbit each other, they will eventually collide, forming a single black hole with a mass less than the sum of the two initial masses. This missing “mass,” up to ten percent, is converted into gravitational waves (GW) making these systems one of the most energetic in the universe. In the last decade, numerical simulations of the coalescence of binary black hole spacetimes have become a possibility and have since then progressed. Each simulation, with a unique set of initial parameters, constructs a gravitational wave signal, also called a waveform. In this work, I study the modeling of the radiated energy of non-precessing and precessing systems as functions of the binary system’s initial parameters. Because constructing a template bank of these waveforms remains computationally intensive, the next step is to introduce the use of Principal Component Analysis (PCA), which will efficiently capture the essential features over a large parameter space of the simulations. It acts on collections of waveforms to find bulk features such as the energy and momentum radiated. These features may provide the “smoking gun” of mergers for gravitational wave burst detection.

# CHAPTER I

## INTRODUCTION

Now that LIGO - called Advanced LIGO [1] - has become more sensitive to a wider range of frequencies, we are closer to detecting the first gravitational waves - whether from supernovae or a compact binary. The detection of these signatures will open a new field in astronomy since we will be able to get an image of the gravitational wave sky for the first time. In preparation for this groundbreaking detection, numerical relativists have been analyzing theoretical waveforms and trying to recover as much information as possible from these signals.

However, it took several decades to solve for dynamical spacetimes [2]. Solving this complex and computationally intensive systems gives numerical relativists a better understanding of the nine dimensional parameter space by outputting waveforms. These waveforms are theoretical gravitational wave signals that allow us to extract initial and final parameters of binary black hole systems. However, each system has a different solution, or waveform, that depends on the initial parameters of the system such as mass, spin, eccentricity, separation distance, etc. Distinguishing between waveforms is nontrivial, and there are several methods that compares them. These methods include match filtering, burst search, and PCA.

The oldest and most developed method is match filtering. A bank of GW templates is created and used for detection by comparing the measured signal with the theoretical counterpart. Not only is this method computationally expensive but it also requires a large amount of time to output results since the algorithm must search the entire template bank before finding the best match [3]. This is a problem because quick recognition of the source is necessary since there are different telescopes that work together with GW observatories, such as Swift and Fermi [4]. Although match filtering works better for mass ranges of 25-100



$M_{\odot}$ , it is better to use burst searches for a higher mass range such as the 100-350  $M_{\odot}$  [5]. Burst searches simply look at an excess of energy in the waveform spectrogram, which is a way of visualizing frequency and power. This method has been employed in recent years as means to look at bulk features. However, it's difficulty lies in finding the optimal resolution since it varies depending on the number and length of the time windows. By acquiring a resolution in the frequency domain, resolution in the power domain is lost and vice-versa.

Although both of the methods mentioned above work well in identifying black hole (BH) parameters, a faster method must be employed in order to get a full glimpse of an coalescence event along with other telescopes. Principal Component Analysis is a tool that acts on collections of waveforms to find bulk features such as the energy radiated and also other black hole parameters like spin and mass [6]. These features are the "smoking gun" of mergers in which we can rely for GW detection. Because this method is not a detailed analysis like match filtering, computational time and, in turn, computational expense decreases. This leads us to quicker detection of GWs.

## CHAPTER II

### NUMERICAL RELATIVITY

#### *2.1 What is Numerical Relativity?*

Numerical relativity is a field in physics that focuses on dynamical spacetimes in the strong-field regime. These spacetimes are affected by compact objects like black holes and neutron stars that emit gravitational radiation. Solving for Einstein's equations is a difficult task that requires intensive use of supercomputers. Not only are the equations challenging by nature - since they are nonlinear, coupled, partial differential equations - but also the parameter space is very large. Its importance also lies in the fact that it picks up where post-Newtonian and perturbation theory break down, such as in the merger of two black holes.

Although numerical relativity began in the 1950s, it took until 2005 to solve the merger of two black holes. Because the choice of coordinates can cause singularities in the equations, it is a very intricate process. One has to be able to choose coordinates that only cause physical singularities, which then present another problem. In order to solve for these types of systems, there has to be a specific technique used to avoid encountering these spacetime singularities [7].

The 2005 breakthrough paper reports on results of binary black hole spacetimes using generalized harmonic coordinates, which was a recently introduced numerical method. The code used has the Einstein field equation in the form of harmonic coordinates and includes a constraint-damping term, which helps the simulations run for longer with a reasonable accuracy. Other features include a discretization scheme, a compactified coordinate system, adaptive mesh refinement, dynamical excision, addition of numerical dissipation, and time slicing to slow down collapse. The results indicate that approximately 5% of the final black holes mass is radiated in the form of GWs.

The weakness presented then was the lack of resolution for the evolution of the binary

black hole spacetimes. Far away from the binary, the estimate of the energy emitted loses accuracy. Once the black holes collide, the energy emitted can be different depending on the extraction radii. At high radii, the resolution is too low while at smaller radii the extraction points are too close and might not be valid in that region. Also, the scalar fields that created the black holes do not all fall into the black holes; thus, leaving noise in the GW signal. This spurious radiation is not necessarily bad, as it vanishes early on and leaves the merger waves unaffected. Finally, the method used to calculate the energy emitted is exposed to numerical error since it sums a positive and finite quantity over time to give  $\frac{dE}{dt}$ . This error inflates the results. However, in order to reduce for this error higher modes can be ignored.

Although earlier methods used excision and a co-rotating shift, the puncture method became more commonly used since it shows fourth order convergence of waveforms at high resolutions and is able to calculate the energy and angular momentum radiated [8]. The numerical methods used here open the possibilities to study binary black hole collisions with a greater extraction radius, unequal masses, and high spins. For this reason, numerical relativity is an evolving field that aims to develop algorithms to solve for astrophysically realistic systems as opposed to highly symmetric, idealized systems. It is a tool necessary to better understand the phenomena occurring in our universe.

## 2.2 *Einstein's Equations*

Black holes are regions of extreme spacetime curvature described by

$$R_{\mu\nu} = -\frac{1}{2}Rg_{\mu\nu} = 8\pi GT_{\mu\nu}. \quad (2.1)$$

The equation above, the so-called Einstein Field Equation, simply tells us something about how the spacetime curvature is shaped by the presence of matter and energy and vice-versa. As complicated as this is mathematically, black holes are considered simple objects in the sense that they are described by three intrinsic parameters, namely charge, spin, and mass. However, the research presented here focuses on black holes in vacuum, meaning that there are no particles and consequently, there is no build up of charge on the system. In theory, there can be non-spinning black holes, but in the universe, it is expected that one would

only see spinning black holes since non-spinning systems would require a very specific and unlikely set of initial conditions. Astrophysically, the spin of the system is defined from zero to one hundred percent of the maximum possible spin. In numerical relativity and gravitational wave physics, the spin,  $a$ , is normalized from zero to one, where  $a = 0$  defines a non-spinning system and  $a = 1$  defines a system spinning at its maximum capacity. Instead of treating black holes with specific masses, mass ratios,  $q$ , are used since they can be applied to any general system.

[material taken from Tower\_Draft.docx]

### 2.3 *Gravitational Waves*

Gravitational waves are small perturbations, or oscillations, in the fabric of spacetime caused by accelerating, nonspherical masses. Because compact objects tend to be very massive, they can readily create larger distortions in spacetime. When two of these objects rotate around their common center of mass, they are accelerating, and thus create gravitational waves with amplitudes larger than less massive objects. These amplitudes are extremely important since they make the signal more easily detectable. Compact objects include black holes, neutron stars, and white dwarfs.

Just as spacetime is generally described by the metric  $g_{\mu\nu}$ , gravitational waves are specifically described by the perturbation metric  $h_{\mu\nu}$ . Therefore, a spacetime with linearized gravitational waves can be described by

$$g_{\mu\nu} = \eta_{\mu\nu} + h_{\mu\nu}, \quad (2.2)$$

where  $\eta_{\mu\nu}$  is the flat spacetime metric, also called Minkowski spacetime. Solutions to the linearized Einstein produce what are called linearized gravitational waves. Given this approximation, it can be shown that they travel at the speed of light, and that they are transverse with two polarizations.

As mentioned above,  $h_{\mu\nu}$  are metric perturbations, and its spacetime can be expressed as

$$ds^2 = -dt^2 + [1 + f(t - z)]dx^2 + [1 - f(t - z)]dy^2 + dz^2, \quad (2.3)$$

where the a function  $f(t - z)$  is needed for the wave to travel in some direction, in this case the  $z$ -direction. Because we have taken these waves to be linearized, we are able to write them as a sum that corresponds to different polarizations. The two polarizations, plus (+) and cross ( $\times$ ) are offset by  $45^\circ$ . By summing up both of the polarizations we are able to get a general gravitational wave of the form

$$h_{\mu\nu}(t, z) = \begin{pmatrix} 0 & 0 & 0 & 0 \\ 0 & f_+(t - z) & f_\times(t - z) & 0 \\ 0 & f_\times(t - z) & -f_+(t - z) & 0 \\ 0 & 0 & 0 & 0 \end{pmatrix}$$

where  $f_+$  and  $f_\times$  are different functions. [used Hartle ch. 16]

## 2.4 Gauge Transformation

The importance of choosing coordinates lies in the simplification of the solution of the linearized Einstein equation. Therefore, we must consider the following coordinate transformation

$$x'^\alpha = x^\alpha + \xi^\alpha(x), \quad (2.4)$$

where  $\xi^\alpha(x)$  is an arbitrary function of the size of a small perturbation, which is correct to first order. We also know that the metric can be transformed as

$$g'_{\mu\nu}(x') = \frac{\partial x^\gamma}{\partial x'^\mu} \frac{\partial x^\delta}{\partial x'^\nu} g_{\gamma\delta}(x). \quad (2.5)$$

With this transformation, we are able to transform the gravitational wave metric with new perturbations, which gives us the gauge transformation

$$h'_{\mu\nu} = h_{\mu\nu} - \partial_\mu \xi_\nu - \partial_\nu \xi_\mu. \quad (2.6)$$

In order to simplify the form of  $h_{\mu\nu}$ , we can choose  $\xi^\alpha(x)$  so that  $V'_\mu(x) = 0$  is satisfied and the variations in the Ricci curvature become

$$\delta R_{\mu\nu} = \frac{\partial \delta \Gamma_{\mu\nu}^\gamma}{\partial x^\gamma} - \frac{\partial \delta \Gamma_{\mu\gamma}^\nu}{\partial x^\nu} = \frac{1}{2}[-\square h_{\mu\nu} + \partial_\mu V_\nu + \partial_\nu V_\mu] \Rightarrow \delta R_{\mu\nu} = -\frac{1}{2}\square h_{\mu\nu}, \quad (2.7)$$

where  $V_\mu$  is just a combination of perturbations, such that

$$V_\mu = \partial_\gamma h_\mu^\gamma - \frac{1}{2} \partial_\mu h_\gamma^\gamma. \quad (2.8)$$

Because we can assume that the four conditions  $V'_\mu(x) = 0$  are true, we can rewrite the Einstein equation as  $\delta R_{\mu\nu} = 0$ , which gives us the wave equation  $\square h_{\mu\nu}(x) = 0$  with the Lorentz gauge condition [9]

$$V_\mu(x) \equiv \partial_\nu h_\mu^\nu(x) - \frac{1}{2} \partial_\mu h_\nu^\nu(x) = 0. \quad (2.9)$$

## CHAPTER III

### ENERGY RADIATED

#### 3.1 *Theoretical Derivation*

In order to derive the change in the energy radiated of a binary black hole system with respect to time, we must first solve the flat-space wave equation for a scalar  $f(x)$ , which is

$$\square f(x) \equiv \eta^{\mu\nu} \frac{\partial^2 f}{\partial x^\mu \partial x^\nu} = -\frac{\partial^2 f}{\partial t^2} + \nabla^2 f = 0 \quad (3.1)$$

and has a solution of the form

$$f(x) = a e^{i\mathbf{k} \cdot \mathbf{x}}, \quad (3.2)$$

where the real part is a physical solution. This means that we can recast this solution for each component of the gravitational wave perturbation such that

$$h_{\mu\nu}(x) = a_{\mu\nu} e^{i\mathbf{k} \cdot \mathbf{x}}. \quad (3.3)$$

Here  $a_{\mu\nu}$  is simply the amplitude components of the gravitational wave. However, they must satisfy the Lorentz gauge conditions. This gives us the power to allow for more transformations of  $\xi_\mu(x)$  as long as our conditions are still satisfied. This leads us to find that  $\square \xi_\mu(x) = 0$ . Additionally,  $h_{\mu\nu}(x)$  satisfies the wave equation, so we can make any of the four equations vanish. We know that the gravitational field has two degree of freedom so we choose a gauge that has two unknown functions, such as the two polarizations. This is called the transverse-traceless gauge, which sets the conditions  $h_{0\mu} = h_i^i = 0$ . This leads us to the perturbation tensor

$$h_{\mu\nu}^{TT} = \begin{pmatrix} 0 & 0 & 0 & 0 \\ 0 & h_+ & h_\times & 0 \\ 0 & h_\times & -h_+ & 0 \\ 0 & 0 & 0 & 0 \end{pmatrix}$$

In general relativity, there is no local expression for the energy of the gravitational field [?]. Therefore, we use the Isaacson stress-energy tensor:

$$T_{\mu\nu} = \frac{1}{32\pi} \langle \partial_\mu h_{ij}^{TT} \partial_\nu h_{ij}^{TT} \rangle = \frac{1}{16\pi} \langle \partial_\mu h_+ \partial_\nu h_+ + \partial_\mu h_\times \partial_\nu h_\times \rangle, \quad (3.4)$$

which averages the energy radiated over a few wavelengths. However, it is important to note that this tensor is only valid for the transverse-traceless gauge. It can be written more compactly as

$$T_{\mu\nu} = \frac{1}{16\pi} \text{Re} \langle \partial_\mu H \partial_\nu \bar{H} \rangle, \quad (3.5)$$

where  $H = h_+ - ih_\times$  and  $\bar{H}$  is the conjugate. Using this equation we are able to find the flux of energy radiated. We can find it along the radial direction such that

$$\frac{dE}{dt dA} = T^{0r} = \frac{1}{16\pi} \text{Re} \langle \partial^0 H \partial^r \bar{H} \rangle = -\frac{1}{16\pi} \text{Re} \langle \partial_t H \partial_r \bar{H} \rangle. \quad (3.6)$$

This can be simplified by using the relation  $\partial_r h = -\dot{h}$  to

$$\frac{dE}{dt dA} = \frac{1}{16\pi} \langle \dot{H} \dot{\bar{H}} \rangle = \frac{1}{16\pi} \langle |\dot{H}|^2 \rangle, \quad (3.7)$$

which gives us the total flux of energy

$$\frac{dE}{dt} = \lim_{r \rightarrow \infty} \frac{r^2}{16\pi} \oint |\dot{H}|^2 d\Omega \quad (3.8)$$

when integrating over the whole sphere. Here,  $d\Omega$  is the standard solid angle element.

In order to characterize spacetime, there needs to be scalars that can be expressed as projections onto a null tetrad of the Weyl tensor, which tells us the tidal force that a body experiences as it moves along a geodesic. The Weyl scalar we are concerned about is  $\Psi_4$  because it describes the outgoing gravitational radiation. In fact, we are able to write  $H$  in terms of  $\Psi_4$  as

$$\Psi_4 = -(\ddot{h}_+ - i\ddot{h}_\times) = -\ddot{H}. \quad (3.9)$$

The other Weyl scalars vanish and we are able to write

$$H = - \int_{-\infty}^t \int_{-\infty}^{t'} \Psi_4 d'' dt'. \quad (3.10)$$



We can use this equation to write the energy radiated in terms of  $\Psi_4$ , but first, we should project it into a sphere to find the angular dependence in terms of the spin-weighted spherical harmonics  ${}_sY^{l,m}$ . Knowing that  $s = -2$  we can expand  $\Psi_4$  as

$$\Psi_4 = \sum_{l=2}^{\infty} \sum_{m=-l}^l A^{l,m} ({}_2Y^{l,m}(\theta, \phi)), \quad \text{where} \quad A^{l,m} = \oint \Psi_4 ({}_2Y^{l,m}(\theta, \phi)) d\Omega. \quad (3.11)$$

Notice that the sum starts at  $l = 2$  since the harmonics are defined for  $l \geq |s|$ . Using our previous equation for  $\frac{dE}{dt}$ , the relation between  $H$  and  $\Psi_4$ , and the orthogonality of the spin-weighted spherical harmonics, we can rewrite our energy radiated as

$$\frac{dE}{dt} = \lim_{r \rightarrow \infty} \frac{r^2}{16\pi} \oint \left| \int_{-\infty}^t \Psi_4 dt' \right|^2 d\Omega = \lim_{r \rightarrow \infty} \frac{r^2}{16\pi} \sum_{l,m} \left| \int_{-\infty}^t A^{l,m} dt' \right|^2. \quad (3.12)$$

This equation tells us to integrate over all time and all modes in order to get the total energy radiated from a given system.

### 3.2 Additional Corrections

Recently, corrections to the estimation of the energy radiated have been calculated by using an improved extrapolation formula for  $r\Psi_4^{l,m}|_{r=\infty}$  [?]. This gives us:

$$\begin{aligned} \frac{dE}{dt} = \frac{1}{16\pi} \sum_{l,m} \left[ \left( 1 - \frac{4M}{r} \right) \left| \int dt \Phi_{l,m} \right|^2 + \frac{(l-1)(l+2)}{2r^2} \left| \iint dt dt' \Phi_{l,m} \right|^2 \right. \\ \left. - 4a \left( \frac{C_{l,m}^{l+1m}}{l+1} \Im \left( \Phi_{l+1m} \left( \int dt \Phi_{l,m} \right) \right) - \frac{C_{l,m}^{l-1m}}{l} \Im \left( \Phi_{l-1m} \left( \int dt \Phi_{l,m} \right) \right) \right) \right], \end{aligned} \quad (3.13)$$

where  $\Phi_{l,m} = r\Psi_{4,l,m}^{NR}(t, r)$  and

$$C_{l,m}^{l',m'} = \int d\Omega {}_2Y_{-2}^{l,m}(\Omega) \cos\theta {}_2Y_{l',m'}^{l',m'}(\Omega). \quad (3.14)$$

This second order corrections promise results closer to the expected value of the energy radiated at a finite extraction radii with an increasing resolution.

## CHAPTER IV

### DETECTION METHODS

#### 4.1 *LIGO*

In order to detect gravitational waves, scientists have engineered a state-of-the-art laser interferometer known as LIGO. LIGO stands for Laser Interferometer Gravitational-wave observatory, and it is a Michelson interferometer. The setup, shown in Figure 4.1, consists of two four kilometers arms that are perpendicular to each other. Because gravitational waves are extremely weak, the arms are in ultra high vacuum. A laser beam is shot into a beam splitter that then transmits half of the light to the end of one arm and reflects the other half of the light to the other arm, where a mirror hangs and reflects the light back. This light is, then, recombined to form a destructive interference pattern. In order for interference to be constructive, there needs to be a change in the length of one of the arms. Because these arms are four kilometers long LIGO is aiming to detect a change in length of  $10^{-18}$  meters which is  $1000^{th}$  the diameter of a proton. Additionally, the end mirrors in LIGO are in a very intricate suspension system in order to reduce several types of noise. The seismic isolation system works in order to reduce any noise that comes mostly from humans, such as forest logging, trains passing, and sport events. Another main noise source is thermal noise from the collision of photons in the mirror. The suspension system for Advanced LIGO consists of a quadruple pendulum with fibers made from silica, which is a material that has a low mechanical loss.

In addition to the LIGO detectors located in the states of Louisiana and Washington in the United States, there are others throughout the world, such as Virgo in Italy and GEO600 in Germany, and currently KAGRA is being built in Japan. A proposal for building one in India has been recently accepted but the construction site has not been chosen yet. The importance of having a network of detectors is that they aid in a method called triangularization, which aids in finding the sky location of the incoming gravitational waves.

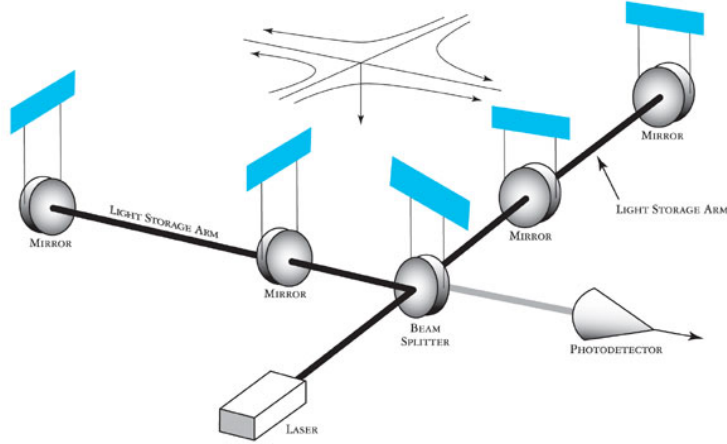


**Figure 4.1:** Basic schematic of the LIGO interferometer.

Also, LIGO needs to rely on multiple detectors in order to correctly identify a gravitational wave since there is a lot of noise in the system.

## 4.2 *Matched Filtering*

Matched filtering is the routine technique that LIGO uses for detection. This method requires the creation of a large bank of waveforms, which run over a large parameter space. Even though we can extract a lot of information from such waveforms, or signals, each simulation can take weeks to months to run. The pace of the simulation depends on factors such as resolution and parameters chosen. For example, simulating a high mass ratio system requires a lot more computational time and resources. Additionally, employing match filtering can take a long time since it consists of trying to “match” a waveform to a detected signal, and, in this way, we are able to extract a lot of information about the initial and final system of binary black holes.

## 4.3 *Principal Component Analysis*

Instead of using the method of matched filtering to match GW signals to signals in a constructed waveform bank, groups in the LIGO Scientific Collaboration (LSC), such as the one at Georgia Institute of Technology, are using a new tool called Principal Component Analysis (PCA). PCA aims to know whether these signals exhibit bulk features for quick detection. This is accomplished by computing the relative probability that a signal belongs

to a specific waveform catalog using Bayesian model selection. This tool is highly effective since the older technique of matched filtering is time consuming and computationally expensive, especially when the simulations include features like high spins, precessing orbits, eccentricity, and changing angles of spin vectors.

# CHAPTER V

## RESULTS

My research focuses on gravitational radiation from binary black hole collisions. Because these waveforms come from the vacuum solution to Einstein's equation, there are only two main intrinsic parameters in our systems, namely mass and spin. The Maya code [10], which solves the initial value problem of Einstein's equations, generates the theoretical gravitational wave data for a range of the physical black hole parameters. The challenge is to recognize patterns in the data that reveal how the information about the originating binary is encoded on the gravitational waves over the nine dimensional parameters, i.e. the two masses, the two spin vectors, and eccentricity of the orbit. The motivation of this project is to provide theoretical models of the gravitational radiation resulting from the merger of the black holes. These models are necessary in detecting the gravitational radiation signal embedded in the noise.

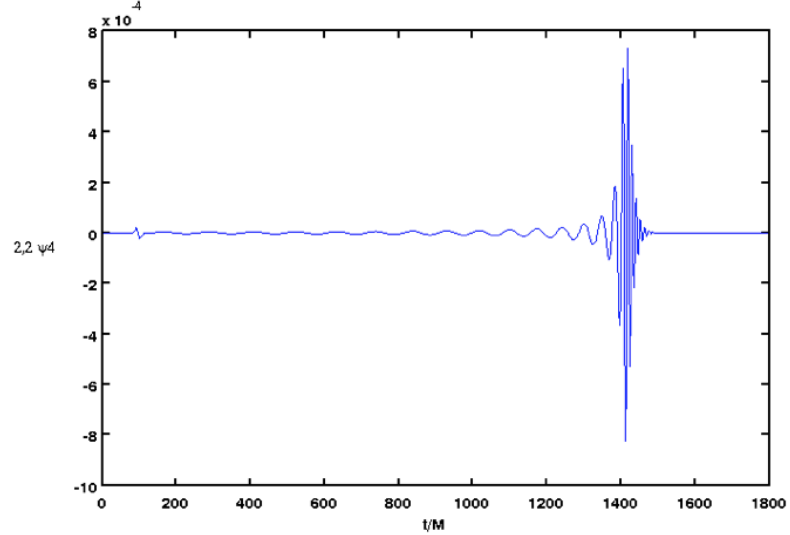


**Figure 5.1:** A gravitational waveform where the y-axis represents the gravitational wave amplitude and the x-axis represents the time evolution of the binary black hole system merging.

Figure 5.1 shows the amplitude of the gravitational radiation as a binary black hole system inspirals, merges, and coalesces. Most of the energy radiated comes from the merger stage. However, this waveform is for the  $l = 2, m = 2$  mode. Different modes have slightly different waveforms. Once the modes are high enough, the waveforms start losing this generic shape since the numerical error increases.

## 5.1 *Non-Precessing Binaries*

We begin by looking at non-precessing systems. That is, systems where the black holes merge in the same plane. Then we look for timescales associated with merger in how the energy is radiated. In order to learn how initial parameters affect the energy radiated, the first waveforms used were from non-spinning systems but with varying mass ratios. We found that with increasing mass ratio, the energy radiated decreases, as shown in Figure 5.2. This makes sense conceptually since the smaller black hole is rotating around the larger black hole, and once it merges the larger black hole will not be perturbed as much. Moreover, we found that increasing the spin of the system increases the radiation.

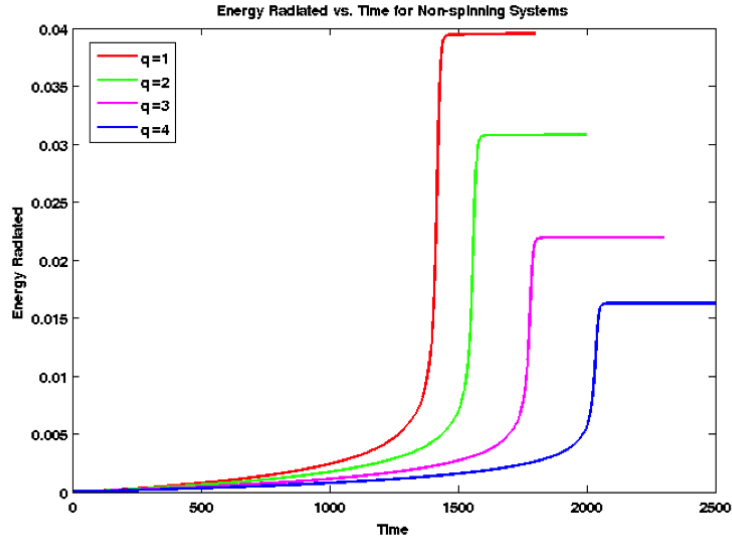


**Figure 5.2:** The energy radiated by mass ratio,  $q$ .

Additionally, the waveforms were decomposed into modes in order to understand how this is imprinted on the gravitational waves. As mentioned in the derivation of the energy radiated,

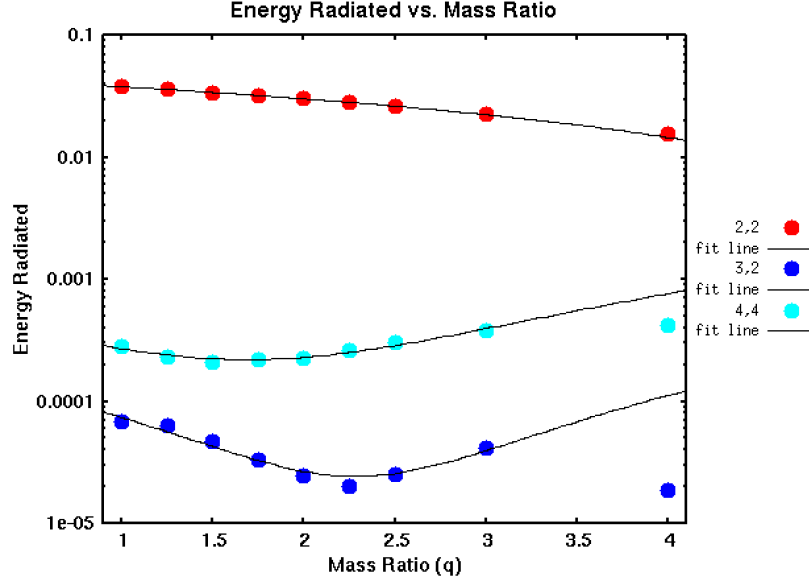


**Figure 5.3:** Energy decomposed into the three most dominant modes for non-spinning systems with a curve fit used for extrapolation.

these modes come from the spin-weighted spherical harmonics that allow us to recast the radiation from a function of  $\theta$  and  $\phi$  into a function of  $l$  and  $m$ . The first mode for gravity is quadrupolar and for inspiraling binaries, the (2,2) mode dominates substantially over all others. Using the radiated energy equation derived above, we are able to calculate the energy radiated into the different modes -  $l$  and  $m$ , where  $m \leq |l|$ . The amplitude of the gravitational wave,  $A^{l,m}$ , is a function of  $(t, l, m)$ . Decomposing the radiation into modes gives a clear physical picture of how the binary is radiating energy. Figure 5.3 depicts the energy radiated per mode per mass ratio. As expected, the energy radiated decreases with an increasing mass ratio. Additionally, it shows how the (2,2) mode dominates by far. Fitting a line to the (2,2) mode, we are able to extrapolate for larger mass ratios - an important result since the numerical challenge increases substantially with increasing mass ratio. The Figure 5.3 shows how the (2,2) mode is the only one that monotonically decreases with an increasing mass ratio while the other modes contain turning points. Two other interesting modes to look at are (3,2) and (4,4). As seen below, they both turn on and off at different mass ratios, but more importantly a decrease in one tends to “trigger” an increase in the other. This effect is more noticeable with higher modes. This turning off

and on can be traced back to the initial values of the parameters and the symmetry they cause.

## 5.2 Precessing Binaries

We found that equal mass, spin-aligned systems radiate the most energy. However, we know this is true for non-precessing systems. Does this indicate that a system prefers to radiate in a certain configuration? Not necessarily. We can test this by studying precessing systems with unequal mass ratios. In order to see how the energy is radiated in precessing systems, we apply similar methods as before. Saying that a system precesses means that the plane of the binary “wobbles.”

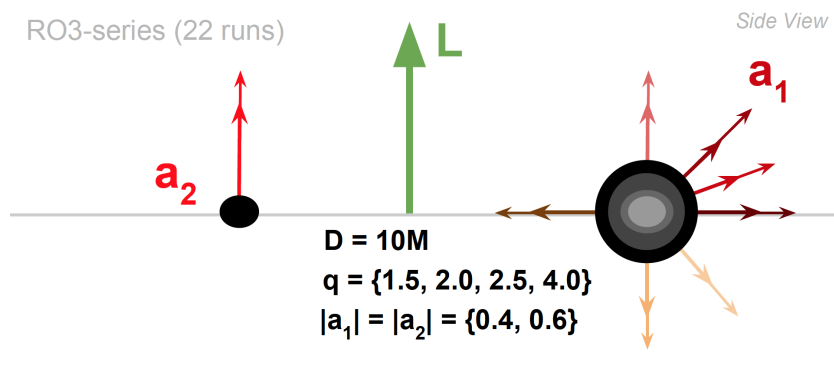


**Figure 5.4:** Sketch of the initial parameters for a given spacetime setup and all the varying parameters, such as mass ratio  $q$ . The colors represent different spin angles but same spin magnitudes  $a_1$  and  $a_2$ .

Figure 5.4 is a sketch of the main setup for the RO3-series catalogue of waveforms we have analyzed. In these systems, we define the lighter black hole to have a spin aligned to the initial angular momentum and the other black hole with a spin making an angle with the z-axis in the xz-plane. The systems we have studied in this catalogue have a spin of 0.6. We vary the mass ratios and find that the results, shown in Figure 5.5, are similar to those of non-precessing systems. However, less energy is radiated when the system precesses about some angle greater than zero.



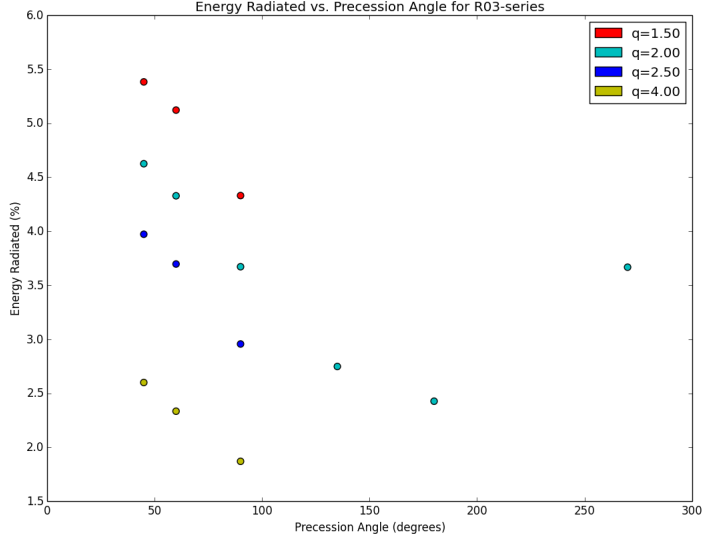


**Figure 5.5:** Energy radiated by mass ratio with a varying precession angle for systems of spin 0.6 with only the spin vector of the larger black hole changing.

We are able to see the dependence of the energy radiated on the precession angle and mass ratio, which forms a v-shape due to the symmetry of the system. We can conclude that the farther the two black holes are from having an aligned spin, the smaller the percentage of the energy radiated from the system.

The next system we analyze is the Lq-series, which consists of changing the precession angles of both black holes, as shown in Figure 5.6. In these systems both black holes have equal magnitude but opposite pointing spin vectors - represented by the colored arrows. For each simulation, we choose the same colors for black holes as the initial parameters and evolve the system in time.

Figure 5.7 shows the results of these systems. Because this catalogue has waveforms with more precessing angles, we are able to see the v-shape more clearly. This is simply due to the symmetry of the system. At  $180^\circ$  we expect very little energy to be radiated; this is represented by the dip in the curve. As the spins become more aligned with the angular momentum of the system, more energy is radiated.

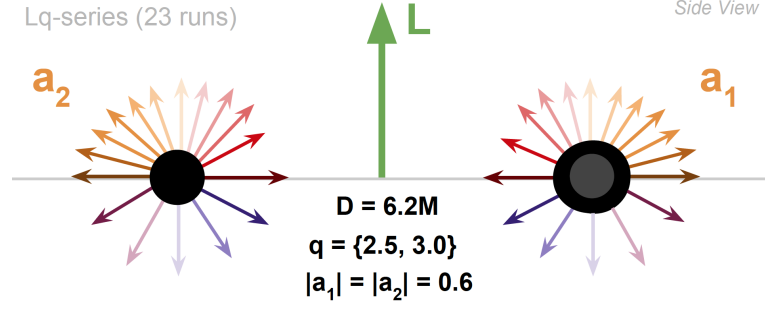


**Figure 5.6:** Sketch of the initial parameters for a given spacetime setup and all the varying parameters, such as mass ratio  $q$ . The colors represent opposite spin angles but same spin magnitudes  $a_1$  and  $a_2$ .

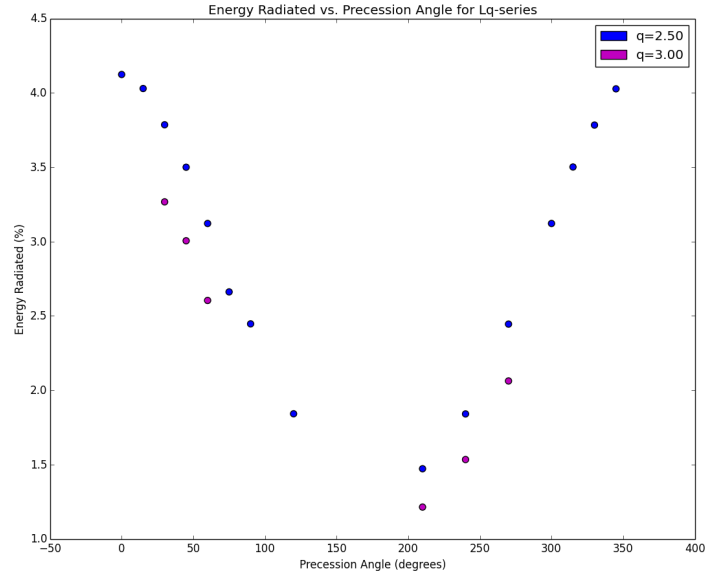


**Figure 5.7:** Energy radiated by mass ratio with a varying precession angle for systems of spin 0.6 with spin vectors of each black hole pointing in opposite directions.

We are then able to compare both precessing systems for similar parameters. For example, comparing the  $q = 2.50$  of both spacetime setups, we can see that less energy is radiated when the system has the angle distributed between both black holes rather than one black hole having an angle on its spin as in Figure 5.7.

## CHAPTER VI

### CONCLUSIONS & FUTURE WORK

The results above become important since they provide a theoretical model for extrapolating parameters. For example, spacetimes with very high mass ratios become very computationally intensive in the sense that simulations begin taking a long time to evolve, which in turn becomes very expensive. Being able to provide a model to extrapolate for higher mass ratios will save resources and allow us to delve deeper into understanding how the energy radiated depends on the geometry of these spacetimes. Additionally, this project provides a foundation for future gravitational wave detection, which is likely to happen within the next two years.

To increase the efficiency of this type of analysis we are looking to use Principal Component Analysis. With this method we will be able to see bulk features encoded in the gravitational waves in a record amount of time. Although it is important to learn all the details from a system, being able to quickly analyze these systems saves time and computational resources. Additionally, current methods of cataloguing waveforms take a long time since it involves comparison of thousands of waveforms. However, using the new method will decrease time spent looking for similar waveforms in order to describe the system of a detection. Being able to have a quick process to extract the information from the gravitational waves will allow us to quickly analyze the data and scrutinize over results that we may find surprising. In this way, new physics might be uncovered and we will be able to see the universe via gravitational waves for the first time.

## REFERENCES

- [1] G. M. Harry and t. L. S. Collaboration, “Advanced LIGO: the next generation of gravitational wave detectors,” *Classical and Quantum Gravity* **27**, 084006 (2010).
- [2] F. Pretorius, “Evolution of Binary Black Hole Spacetimes,” *Physical Review Letters* **95** (2005), arXiv: gr-qc/0507014.
- [3] J. Healy, P. Laguna, and D. Shoemaker, “Decoding the final state in binary black hole mergers,” *arXiv:1407.5989 [astro-ph, physics:gr-qc]* (2014), arXiv: 1407.5989.
- [4] A. R. Williamson, C. Biwer, S. Fairhurst, I. W. Harry, E. Macdonald, D. Macleod, and V. Predoi, “Improved methods for detecting gravitational waves associated with short gamma-ray bursts,” *arXiv:1410.6042 [astro-ph, physics:gr-qc]* (2014), arXiv: 1410.6042.
- [5] S. Mohapatra, L. Cadonati, S. Caudill, J. Clark, C. Hanna, S. Klimenko, C. Pankow, R. Vaulin, G. Vedovato, and S. Vitale, “Sensitivity Comparison of Searches for Binary Black Hole Coalescences with Ground-based Gravitational-Wave Detectors,” *Physical Review D* **90** (2014), arXiv: 1405.6589.
- [6] J. Clark, L. Cadonati, J. Healy, I. S. Heng, J. Logue, N. Mangini, L. London, L. Pekowsky, and D. Shoemaker, “Investigating Binary Black Hole Mergers with Principal Component Analysis,” *arXiv:1406.5426 [gr-qc]* (2014), 2007PhRvD..76h4020V: 1406.5426.
- [7] T. W. Baumgarte and S. L. Shapiro, *Numerical Relativity: Solving Einstein’s Equations on the Computer* (, 2010).
- [8] M. Campanelli, C. O. Lousto, P. Marronetti, and Y. Zlochower, “Accurate Evolutions of Orbiting Black-Hole Binaries Without Excision,” *Physical Review Letters* **96** (2006), arXiv: gr-qc/0511048.

- [9] J. B. Hartle and J. Traschen, “Gravity: An Introduction to Einstein’s General Relativity,” *Physics Today* **58**, 52 (2005).
- [10] B. Vaishnav, I. Hinder, F. Herrmann, and D. Shoemaker, “Matched filtering of numerical relativity templates of spinning binary black holes,” *Physics review D* **76**, 084020 (2007) 0705.3829.